Received: 15 September 2022 | Revised: 15 December 2022 | Accepted: 17 December 2022

DOI: 10.1111/cid.13172

ORIGINAL ARTICLE

WILEY

Bioactive glass air-abrasion promotes healing around contaminated implant surfaces surrounded by circumferential bone defects: An experimental study in the rat

Faleh Abushahba DDS, MDentCh, PhD[1] | Nagat Areid DDS, MDentCh, PhD[1] | Mervi Gürsoy DDS, PhD[2] | Jaana Willberg DDS, PhD[3,4] | Varpu Laine DVM[5] | Emrah Yatkin PhD, Dipl. ECLAM[5] | Leena Hupa Dsc(Eng)[6] | Timo O. Närhi DDS, PhD[1]

[1]Department of Prosthetic Dentistry and Stomatognathic Physiology, Institute of Dentistry, University of Turku, Turku, Finland

[2]Department of Periodontology, Institute of Dentistry, University of Turku, Turku, Finland

[3]Department of Oral Pathology and Radiology, Institute of Dentistry, University of Turku, Turku, Finland

[4]Department of Pathology, Turku University Hospital, Turku, Finland

[5]Central Animal Laboratory, Faculty of Medicine, University of Turku, Turku, Finland

[6]Johan Gadolin Process Chemistry Centre, Åbo Akademi University, Turku, Finland

Correspondence
Faleh Abushahba, Department of Prosthetic Dentistry and Stomatognathic Physiology, Institute of Dentistry, University of Turku, Lemminkäisenkatu 2, FI-20520, Turku, Finland.
Email: fafabu@utu.fi

Funding information
State Research Funding, Grant/Award Number: ERVA50036

Abstract

Objectives: The present study aimed to evaluate the healing of experimentally induced bone defects around contaminated dental implants after air-abrasion using 45S5 or zinc oxide (ZnO)-containing bioactive glasses (BAGs).

Materials and Methods: One maxillary first molar was extracted from each Sprague–Dawley rat ($n = 30$). After 4-week healing, a titanium implant was placed in the extraction site with a circumferential bone defect. The rats were randomized into five different groups: (1) implants with *Fusobacterium nucleatum* and *Porphyromonas gingivalis* dual-species biofilm (IB); (2) implants with biofilm subjected to inert glass air-abrasion (inert); (3) sterile implants (S); (4) implants with biofilm subjected to 45S5 BAG air-abrasion (45S5); and (5) implants with biofilm subjected to ZnO-containing BAG air-abrasion (Zn4). After 8-week healing, maxillae were dissected, and histomorphometric analyses were performed.

Results: The first bone-to-implant contact was significantly shorter for the inert (1.58 ± 1.16 mm; $p = 0.016$), S (0.28 ± 0.13 mm; $p < 0.001$), 45S5 (0.41 ± 0.28 mm; $p < 0.001$), and Zn4 (0.26 ± 0.16 mm; $p < 0.001$) groups compared to IB group. Also, significantly more bone-to-implant contact was seen for S (72.35% ± 8.32%; $p < 0.001$), 45S5 (57.91% ± 24.10%; $p = 0.002$), and Zn4 (70.49% ± 12.74%; $p < 0.001$) groups than the IB group. The bone volume with the threads demonstrated significantly higher value for S (69.32% ± 9.15%; $p < 0.001$), 45S5 (58.93% ± 23.53%; $p = 0.001$), and Zn4 (68.65% ± 12.41%; $p < 0.001$) groups compared to the IB group. The bone volume within the defects was significantly higher for S (68.79% ± 11.77%; $p < 0.001$), 45S5 (62.51% ± 20.51%; $p = 0.002$), and Zn4 (73.81% ± 15.07%; $p < 0.001$) groups compared to the IB group.

This work has been conducted at the Institute of Dentistry, University of Turku.

Conclusions: This study suggests that air-abrasion of contaminated moderately rough implant surfaces with either 45S5 or ZnO-containing BAGs enhances osseointegration and bone defect regeneration.

KEYWORDS
bioactive glasses, bone defects, dental implants, *Fusobacterium nucleatum*, peri-implantitis, *Porphyromonas gingivalis*

Summary Box

What is known

- Peri-implantitis can lead to the contamination and the formation of a high-affinity biofilm on the implant surface.
- Various methods are currently used for implant surface decontamination, but no single method was found to be superior in terms of clinical outcomes.

What this study adds

- This animal trial presents evidence that air-abrasion using either 45S5 or ZnO-containing bioactive glasses results in better osseointegration and bone regeneration than implants subjected to inert glass air-abrasion treatment.

1 | INTRODUCTION

Peri-implantitis (PI) is the most common reason for implant failure, with prevalence ranging from 1% to 47%.[1,2] It is accepted that peri-implant diseases are plaque-induced inflammatory diseases induced by the development and establishment of a complex bacterial biofilm structure on the implant surfaces.[3] Peri-implant diseases are classified into peri-implant mucositis and PI, and both diseases share similar clinical features, including bleeding on probing, redness, and swelling in peri-implant mucosa. In addition, PI is also characterized by suppuration and increased pocket depth combined with progressive bone loss after the initial bone remodeling.[4,5]

Exposure of the implant surface to the oral environment can lead to the formation of a high-affinity biofilm that is robust, retentive, and difficult to eradicate.[6] It starts with the adhesion of the initial colonizers, such as oral streptococci, to the acquired pellicle, which facilitates the adhesion of successive colonizers like *Fusobacterium nucleatum*. *F. nucleatum* serves as a bridge between initial and late bacterial colonizers, including the red complex bacterial pathogens, *Tannerella forsythia*, *Treponema denticola*, and *Porphyromonas gingivalis*, which are actively associated with periodontal and peri-implant diseases.[7–13]

The debridement of the implant surface is an essential step in treating peri-implant diseases. However, implant design and surface roughness may facilitate the development and retention of the bacterial biofilm and limit the effectiveness of mechanical debridement.[6,14] The current methods used for cleaning the infected implant surfaces, including curettes, titanium brushes, sonic/ultrasonic instruments, and air-abrasive devices, fail to demonstrate adequate implant surface debridement.[6,14–17] Even though there is no solid clinical evidence suggesting, which modality is the most effective for treating PI,[18] in vitro experiments have shown that air particle abrasion has superior or equal potential for decontamination when compared to other cleaning modalities.[19,20]

Bioactive glasses (BAGs) are a group of biomaterials that can be successfully used in air particle abrasion procedures.[21,22,23] Numerous studies have shown that 45S5 and S53P4 BAGs possess broad-spectrum antimicrobial and antibiofilm effects against a wide range of Gram-positive and Gram-negative oral bacteria.[24–28] The antimicrobial effects of BAG are mainly due to the rise in the pH and local osmolarity caused by Na, Si, and Ca^{2+} ion dissolution.[29] The original 45S5 BAG has been modified by including zinc oxide (ZnO) powder.[30] Experimental Zn-substituted compositions have been shown to produce antibacterial effects with minimal pH increase.[31] The antibacterial effect of the ZnO-containing BAG is attributed to the release of Zn^{2+}, which can penetrate the bacterial cell membrane, resulting in the generation of toxic reactive oxygen species (ROS) and thereby causing bacterial death.[32]

Several studies have used the rat model to evaluate dental implant osseointegration and create a model for PI.[33,34] However, it is not known whether BAG air-abrasion of bacterial biofilm formed on dental implant surfaces can enhance osseointegration in the rat model. This study aimed to evaluate the healing of experimentally induced bone defects around contaminated dental implants after air-abrasion with 45S5 or ZnO-containing (Zn4) BAGs.

2 | MATERIALS AND METHODS

2.1 | Titanium Implants and surface treatment

In this study, a total of 33 Grade 2 commercially pure titanium screws 2.0 mm ∅ × 3.0 mm length (Titanium Service, Vourles, France) were used as dental implants (30 implants used for implantation and

3 implants for SEM images). The implants were surface treated in-house with sandblasting and acid-etching (SA). The SA process was carried out by sandblasting with large grit aluminum oxide particles (250–500 μm) using an air pressure of 5 bar followed by acid-etching in HCl (60%) and H_2SO_4 (70%) acid combination for 1 h at 60°C. Then the titanium implants were thoroughly rinsed with deionized water in an ultrasonic bath for 20 min to eliminate acid residues. Implants were then allowed to dry in a hot air oven for 30 min at 50°C.

2.2 | Dual-species biofilm formation

The dual-species biofilms of *F. nucleatum* (ATCC 25586; the American Type Culture Collection) and *P. gingivalis* (AHN 24155; the Finnish Institute for Health and Welfare) were formed as described previously.[25] Briefly, the 5-day-old pure bacterial cultures were first suspended in tryptic soy broth (TSB; Merck KGaA, Darmstadt, Germany) enriched with hemin (5 mg/L) and menadione (5 mg/L) and then incubated overnight at 37°C in an anaerobic workstation (Don Whitley Scientific Ltd., West Yorkshire, England) with an atmosphere of 85% N_2, 10% H_2, and 5% CO_2.

Implants ($n = 24$) were coated with pasteurized saliva (diluted 1:3 with phosphate-buffered saline [PBS]) at 37°C for 30 min and then rinsed with PBS and transferred to a new 24-well plate. Based on the optical density adjustments (OD 0.5 at 490 nm), equal amounts of both bacterial suspensions (i.e., 2×10^7 colony forming units/ml) in fresh media were distributed to each well and incubated under anaerobic conditions at 37°C for 70 h.

In order to remain the anaerobic atmosphere (85% N_2, 10% H_2, and 5% CO_2) until the implant surgery, the implants were transferred into anaerobic jars (Thermo Fisher Scientific, Waltham, MA, USA) and carried to the Central animal laboratory, PharmaCity, University of Turku, Finland.

2.3 | Scanning electron microscopy

Three other implants (sterile SA, with biofilm and after ZnO-containing BAG air-abrasion) were used for scanning electron microscopy (SEM) imaging. The implants were rinsed three times in deionized water and then fixed in 2.5% glutaraldehyde overnight. The dehydration was performed by using graded ethanol series (50%, 70%, 85%, 95%, and 100%). Before SEM imaging, the implants were sputter-coated with carbon utilizing Emscope TB 500 Temcarb (Thermo VG, Waltham, Massachusetts, USA). The SEM (LEO Gemini 1530 with a Thermo Scientific UltraDry Silicon Drift Detector, Oberkochen, Germany) was used to visualize the implant surfaces.

2.4 | Sample size calculation

The resource equation method described by Charan and Kantharia was used to estimate the required number of experimental animals.[35] This method measures the "E" value that represents the degree of freedom of analysis of variance (ANOVA). The *E* value should be considered adequate between 10 and 20.

$$E = \text{total number of observations} - \text{total number of groups}.$$

$E = (25)–5 = 20$, which is considered an adequate sample size according to Charan and Kantharia.[35] Considering losing animals, for example, during surgery and at the postsurgical period, or implant loss during the healing period, the sample size was increased by 20%, making the total number included in the study 30 rats.

2.5 | Animals and anesthesia

The study protocol was prepared before the study, reviewed and approved by the Regional State Administrative Agency for Southern Finland (license number: ESAVI/26978/2019), and complied with the ARRIVE guidelines. A total of 30 (250–400 g) healthy male Sprague–Dawley rats (Envigo, The Netherlands) were used in the study. The rats were specific pathogen-free, not genetically modified, nor subjected to any previous procedure.

The animals were housed at the Central Animal Laboratory, University of Turku, Finland, and surgeries were carried out in the same premises from February 2021 to May 2021. All the experiments were carried out according to Finnish and European regulations about the care and use of research animals; a veterinarian monitored the rats daily during the study period. Exclusion criteria were set before the start of the experiment. They included weight loss of 20% or more at any time point during the experiment, which also resulted in immediate euthanasia of the rat, implant loss, or death before termination of the experiment. Throughout the study period, all animals were housed in the same room and in a separate cage, maintained at a controlled temperature (21°C ± 3°C) and humidity (55% ± 15%) with access to RM3 Soya-free food and water ad libitum.

Carprofen (Carprolifican vet, Fauna Pharma, the Netherlands) 5 mg/kg was used 30 min before anesthesia and 2 days for post-surgical analgesia. The general anesthesia was conducted with a subcutaneous injection of the anesthetic cocktail, which is composed of Ketamine (Ketaminol, Intervet, Netherlands) 45 mg/kg, Medetomidine (Cepetor vet, Vetmedic, Finland) 0.25 mg/kg, and Midazolam (Midazolam, Hameln Pharma, Germany) 1 mg/kg. Atipamezole hydrochloride (Antisedan vet, Orion Pharma, Finland) 5 mg/ml was used at the end of the surgical procedure to reverse the anesthetic medication.

2.6 | Surgical procedures

All animals underwent two surgical procedures, one for extraction of a first maxillary molar and the other for implantation. After adequate anesthesia, one first maxillary molar was extracted from each animal. The gingival attachment of the tooth was cut around the entire circumference. Then, the tooth was luxated and elevated using a micro

Periotome (Hu-Friedy, Chicago, USA). After a 4-week healing period, the rats were anesthetized again using the abovementioned method, and mucoperiosteal flaps were elevated in order to expose the edentulous maxillary first molar region.

The Central Animal Laboratory personnel randomized the rats into five groups according to different treatments modalities: (1) implants with intact dual-biofilm of *F. nucleatum* and *P. gingivalis* (IB); (2) implants with biofilm subjected to inert glass air-abrasion (inert); (3) sterile implants (S); (4) implants with biofilm subjected to 45S5 BAG air-abrasion (45S5); and (5) implants with biofilm subjected to ZnO-containing BAG air-abrasion (Zn4). The air-abrasion of the implants was performed using an LM ProPower device (LM dental, Parainen, Finland). Before their placement, the implants with biofilm were subjected to air-abrasion using 45S5 BAG, Zn4 BAG, or inert glass, particle size (45–120 μm). The oxide composition and preparation method of BAGs used in this study are described elsewhere.[24] Each implant was air-abraded using 4 bar air pressure for 20 s. The S and IB groups were used as positive and negative controls without air-abrasion treatment.

The osteotomy sites were prepared using 1.0 mm followed by 1.6 mm twist drills under a copious stream of sterile saline. Before the implant placement, bone defects were created in the coronal 1 mm using a 2.4 mm twist drill, which resulted in 0.2 mm circumferential defects (Figure 1). A total of 30 implants (one implant per animal) were used in the implantation procedure: 6 implants in each treatment category. The alveolar mucosa was then sutured using 5/0 absorbable sutures (Coated Vicryl, Ethicon, USA), and the animals were returned to their cages in the same environmental conditions mentioned earlier. After an 8-week healing period, the animals were euthanized in a CO_2 euthanasia chamber, and the maxillae were then harvested. Three implants belonging to the IB group were lost during the experiment, and therefore, they were excluded from the analysis.

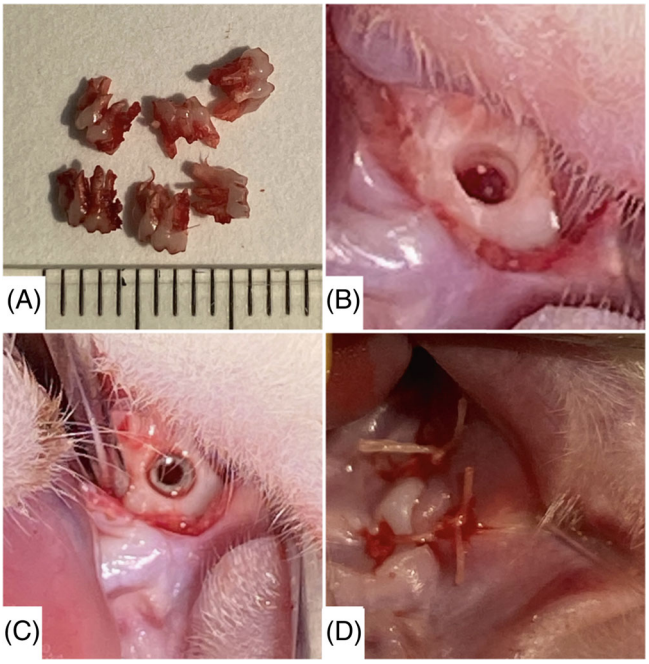

FIGURE 1 Shows representative images for (A) the extracted maxillary first molar teeth, (B) the osteotomy site preparation, (C) implant placement with the circumferential bone defect, and (D) sutures in place

2.7 | Histomorphometric analysis

The maxillae were dissected and immediately placed in 10% formalin for fixation. The obtained specimens were rinsed in distilled water, dehydrated in ethanol, and then preinfiltrated with dilute methyl methacrylate. The specimens were infiltrated using pure methylmethacrylate and polymerized over 14 days. The blocks were then sectioned in a bucco-palatal direction into 100 μm thickness using a diamond band saw (Exakt Technologies, Oklahoma City, OK, USA). The thickness was reduced to 40 μm by grinding the sections with silicon carbide papers of P500, P800, P1200, and P2500 and polished with K4000 (Exakt Technologies). The specimens were finally stained with hematoxylin and eosin (H&E) stain. Two slides were obtained from each block. The slides were visualized using a light microscope (Leitz Aristoplan, Leica Microsystems, Wetzlar, Germany), and the images were captured with a digital camera (Leica DFC, Leica Microsystems). Two masked calibrated investigators (F.A. and N.A.) evaluated all histomorphometric measurements using image analysis software (Fiji® image J2, 2.3.0). The interexaminer correlation coefficient was 0.985 (95% confidence intervals: 0.979–0.989). The analysis was focused on the coronal 1 mm of the implants, and the results are reported as an average of the two examiners' measurements.

The following parameters were evaluated:

1. linear distance from the top of the implant to the highest point of bone to implant contact; first bone-implant contact (FBIC);

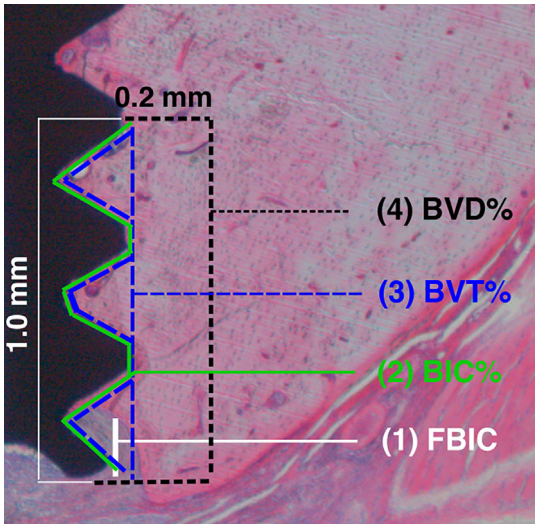

FIGURE 2 Illustrating the histomorphometric measurements made in the coronal 1 mm of the implant: (1) the distance from the implant margin to the first bone-to-implant contact (FBIC), (2) the percentage of bone in contact with the implant (BIC%), (3) the percentage of the bone volume within the threads (BVT%), and (4) the percentage of bone volume within the defect (BVD%).

2. percentage of bone in direct contact with the coronal 1 mm of the implant surface (BIC%);
3. percentage of bone volume within the threads of the coronal 1 mm of the implant (BVT%); and
4. percentage of bone volume within the defect (0.2 mm × 1 mm), (BVD%), (Figure 2).

2.8 | Statistical analysis

Data were expressed in means (±SD), considering the rat as the statistical unit of analysis ($n = 30$). The data were tested for normality by means of a Shapiro–Wilk test. Logarithmic transformation was performed on skewed data to accomplish normal distribution. Statistical analysis was performed using Statistical Package Software IBM SPSS Statistics for Mac, version 28.0 (IBM Corp., Armonk, NY, USA). Pearson correlation coefficient was calculated to evaluate the accuracy of measurements between the two examiners. The statistical significance among the experimental groups was analyzed using ANOVA followed by Tukey's post hoc test. Differences were considered significant at 95% confidence levels, with p values below 0.05.

3 | RESULTS

3.1 | SEM images observations

The SEM images for the SA implant showed that the sandblasting and acid etching of the titanium implants resulted in apparent surface roughness with different crater sizes. The SA titanium implant was well covered with the dual-species biofilms of *F. nucleatum* and *P. gingivalis* after 70 h of incubation (IB). After the biofilm-covered titanium implant was subjected to air-abrasion using Zn4 BAG, no bacterial cells could be detected. SEM images were taken in five randomly selected locations per sample (Figure 3).

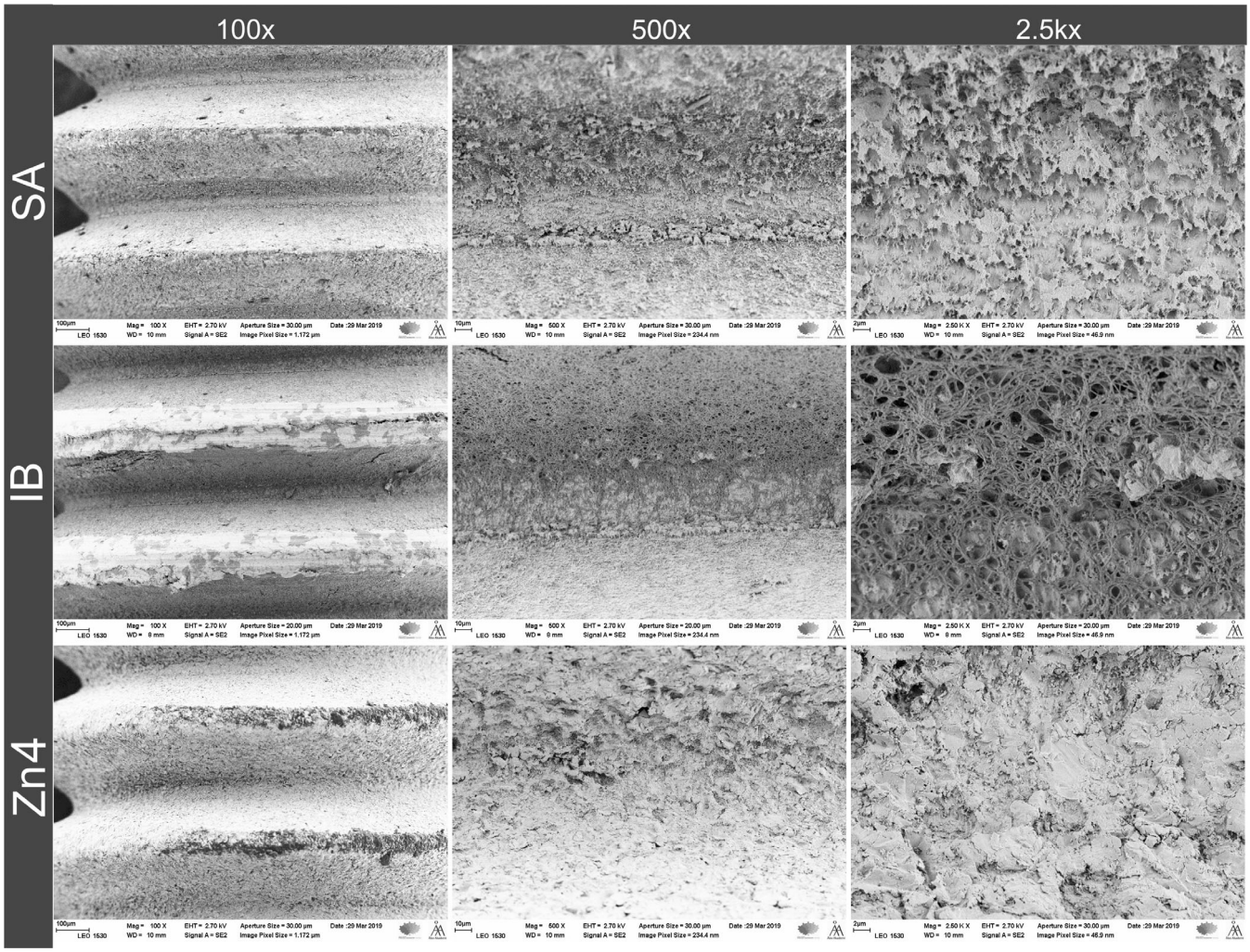

FIGURE 3 SEM images for a sandblasted and acid-etched (SA) titanium implant, an implant with *F. nucleatum* and *P. gingivalis* dual biofilm (IB), and an implant with biofilm subjected to ZnO BAG air-abrasion (Zn4) (magnifications: 100×, 500×, and 2.5k×).

3.2 | Surgical procedures and implant loss

All implants ($n = 30$) were successfully installed, and all the rats survived and recovered quickly from surgery. The animals appeared in good health throughout the experimental period and did not lose weight or show any other adverse reactions. Three implants belonging to the intact biofilm (negative control) group were lost during the healing period.

3.3 | First bone-to-implant contact

The distance from the implant margin to the first bone-to-implant contact (FBIC) showed significant differences among the treatment groups. FBIC was significantly more coronal for the S (0.281 ± 0.132; $p < 0.001$), 45S5 (0.412 ± 0.283; $p < 0.001$), and Zn4 (0.263 ± 0.160; $p < 0.001$) groups compared to IB group. Additionally, the inert group demonstrated a significantly lower value of FBIC (1.582 ± 1.157; $p = 0.016$) than the IB group since the entire surface of IB implants had no bone contact (Figures 4 and 5).

3.4 | Percentage of bone-to-implant contact

The BIC% was significantly higher for the S (72.36 ± 8.32; $p < 0.001$), 45S5 (57.91 ± 24.10; $p = 0.002$), and Zn4 (70.49 ± 12.74; $p < 0.001$) compared to the IB group. The BIC% in the inert group was statistically nonsignificant (16.20 ± 25.53; $p = 0.72$) compared to IB group. No bone in contact with the implant was observed for the IB group (Figures 4 and 6).

3.5 | Percentage of bone volume within the threads

The BVT% showed highly significant differences among groups. The BVT% for the S (69.325 ± 9.154; $p < 0.001$), 45S5 (58.932 ± 23.526; $p = 0.001$), and Zn4 (68.653 ± 12.411; $p < 0.001$) groups were significantly higher than for the IB group. The BVT% in the inert group was statistically nonsignificant (14.90 ± 25.88; $p = 0.775$) compared to IB group. No bone formation within threads was observed for the IB group (Figures 4 and 7).

3.6 | Percentage of bone volume within the defect

The difference in BVD% was highly significant among the groups. The mean BVD% for the S (68.792 ± 11.771; $p < 0.001$), 45S5 (62.507 ± 20.512; $p = 0.002$), and Zn4 (73.812 ± 15.067; $p < 0.001$) groups was significantly higher compared to the IB (5.033 ± 0.929). The BVD % in the inert group was statistically non-significant (17.810 ± 25.029; $p = 0.849$) compared to IB group (Figures 4 and 8).

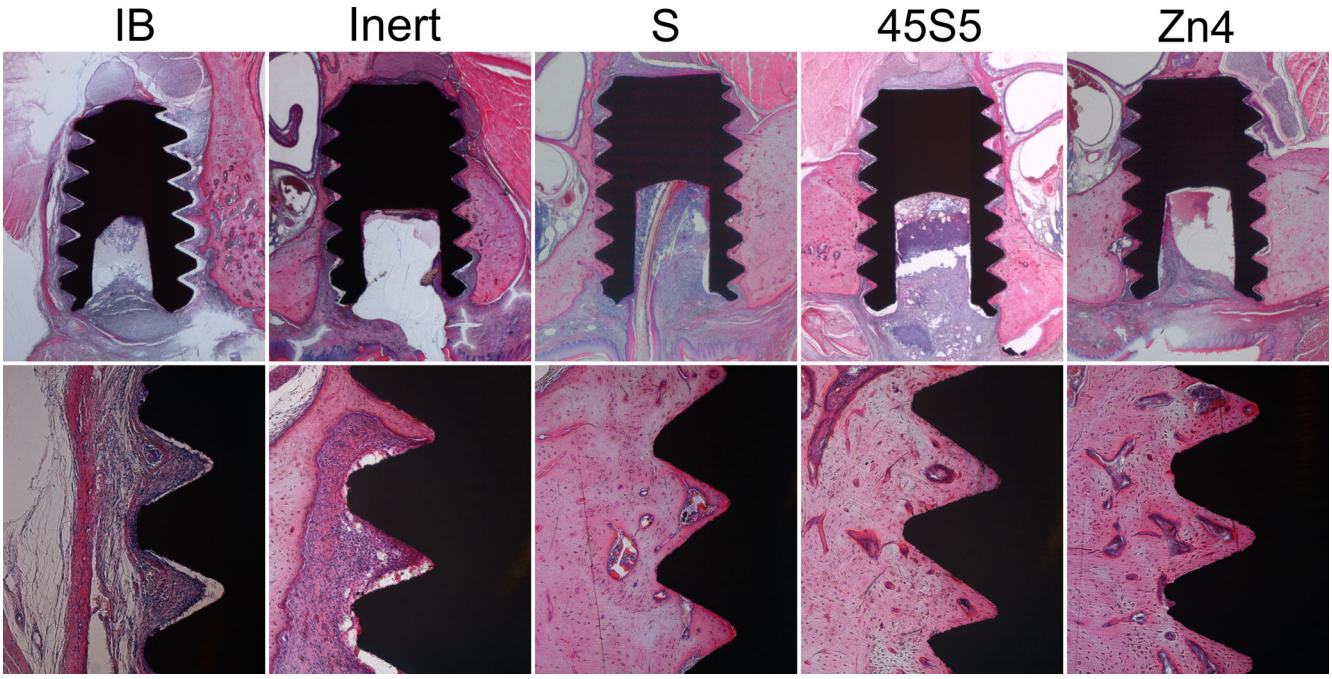

FIGURE 4 Ground histologic section with H&E staining shows the peri-implant situation after 8-week healing at 5× and 10× magnification (IB; implants with *F. nucleatum* and *P. gingivalis* intact biofilm, inert; implants with biofilm subjected to inert glass air-abrasion, S; sterile implant, 45S5; implants with biofilm subjected to 45S5 BAG air-abrasion, and Zn4; implants with biofilm subjected to ZnO-containing BAG air-abrasion). The implant with intact biofilm shows severe inflammatory cell infiltration. The inert glass abraded implant site shows moderate coronal inflammatory infiltrates. S, 45S5, and Zn4 sites demonstrate healthy bone tissue with no sign of inflammation.

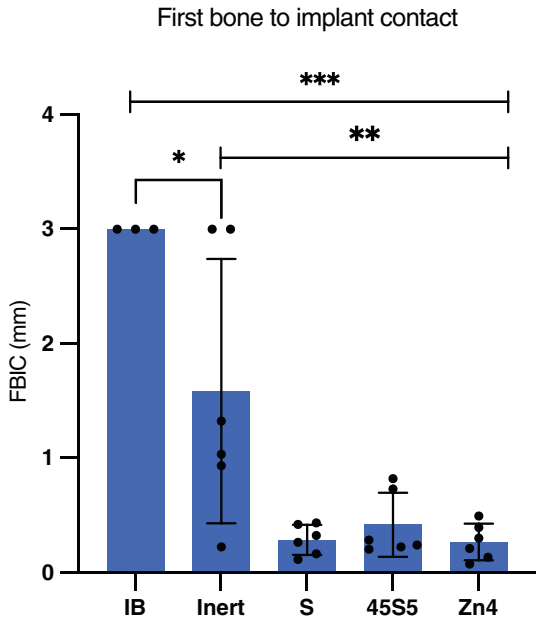

FIGURE 5 Means for linear measurement (mm) of first bone to implant contact (FBIC) per implant modality. (IB; implants with *F. nucleatum* and *P. gingivalis* intact biofilm, Inert; implants with biofilm subjected to inert glass air-abrasion, S; sterile implant, 45S5; implants with biofilm subjected to 45S5 BAG air-abrasion, and Zn4; implants with biofilm subjected to ZnO containing BAG air-abrasion). The dots represent the values of individual measurements. $^{*}p < 0.05$, $^{**}p < 0.01$, $^{***}p < 0.001$

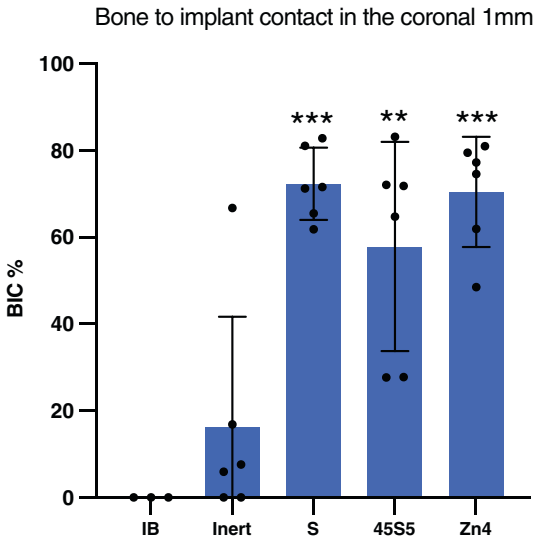

FIGURE 6 Mean percentage of bone-to-implant contact (BIC%) in the coronal 1 mm of the implant per implant modality. (IB; implants with *F. nucleatum* and *P. gingivalis* intact biofilm, Inert; implants with biofilm subjected to inert glass air-abrasion, S; sterile implant, 45S5; implants with biofilm subjected to 45S5 BAG air-abrasion, and Zn4; implants with biofilm subjected to ZnO-containing BAG air-abrasion). The dots represent the values of individual measurements. $^{**}p < 0.01$, $^{***}p < 0.001$

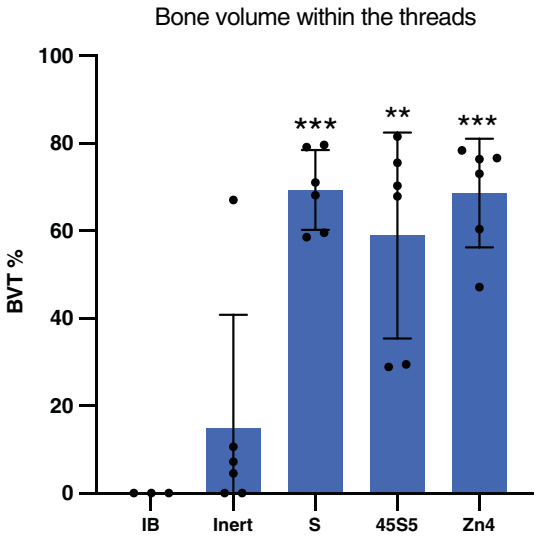

FIGURE 7 Mean percentage of the bone volume within the threads (BVT%) in the coronal 1 mm of the implant per implant modality. (IB; implants with *F. nucleatum* and *P. gingivalis* intact biofilm, Inert; implants with biofilm subjected to inert glass air-abrasion, S; sterile implant, 45S5; implants with biofilm subjected to 45S5 BAG air-abrasion, and Zn4; implants with biofilm subjected to ZnO-containing BAG air-abrasion). The dots represent the values of individual measurements. $^{**}p < 0.01$, $^{***}p < 0.001$.

4 | DISCUSSION

This study aimed to assess the effect of BAG air-abrasion of implant surface bacterial biofilm on osseointegration and healing of experimentally induced bone defects. The histomorphometric analysis revealed that air-abrasion of the implant surface with dual biofilm formed using 45S5 or Zn4 BAGs significantly improved osseointegration and healing of the experimental marginal bone defect. Inert glass air-abrasion resulted in considerably less bone fill and weaker osseointegration. The effect of inert glass air-abrasion is only limited to mechanical cleaning, while the investigated BAGs have an antibacterial effect.[24–28] Furthermore, implants with an intact biofilm fail to osseointegrate and demonstrate severe inflammatory cell infiltration.

The implants treated with Zn4 BAG air-abrasion demonstrated a comparable effect as seen for sterile implants. This is probably related to the Zn^{2+} ion release from the Zn-containing BAG, as demonstrated in our previous study.[31] Zn^{2+} ion is an essential element for the growth, proliferation, and differentiation of osteoblast cells, but it can also stimulate osteoblast cell attachment and inhibit osteoclastic cell activity.[36,37] Moreover, silicate ion release from 45S5 BAG has been shown to play an essential role in stimulating the proliferation and differentiation of osteoblast cells.[38,39]

Implant surface decontamination is a crucial step in treating peri-implant disease. However, the design and surface roughness of the implant may impede the successful eradication of biofilm.[5,14] Previous work by the authors has shown that particulate BAG of particle size (45–120 μm) can be successfully used in air-abrasion applications and demonstrate a consistent and uniform surface topography to the titanium

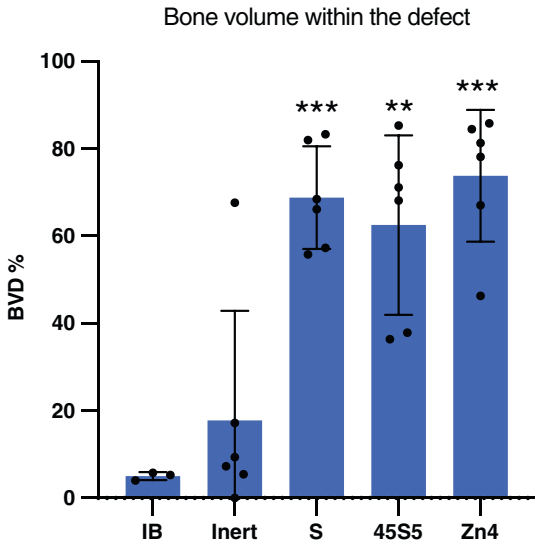

FIGURE 8 Mean percentage of the bone volume within the defect (BVD%) in the coronal 1 mm of the implant per implant modality. (IB; implants with *F. nucleatum* and *P. gingivalis* intact biofilm, Inert; implants with biofilm subjected to inert glass air-abrasion, S; sterile implant, 45S5; implants with biofilm subjected to 45S5 BAG air-abrasion, and Zn4; implants with biofilm subjected to ZnO-containing BAG air-abrasion). The dots represent the values of individual measurements. $^{**}p < 0.01$, $^{***}p < 0.001$

surface.[31] In addition, the air-abrasion process results in BAG particles getting trapped onto titanium surfaces which could impart antibacterial properties to the titanium surface. Air-abrasion of *Streptococcus mutans*, as well as *F. nucleatum* and *P. gingivalis*, formed on SA titanium surface using 45S5 BAG or BAG particle doped with ZnO, could inhibit bacterial growth in laboratory conditions as demonstrated in our previous studies.[24,25] The antibacterial and antibiofilm effects could be explained by Si, Ca^{2+}, and Na ions released from the residual BAG particles on SA surfaces which can cause a local elevation in the pH.[29,40] Nevertheless, dissolution of Zn-containing BAG results in a minimal elevation in the pH.[31,41] Therefore, its antibacterial effect cannot be explained solely by the increase in the pH. Besides the antibacterial effect of BAG, the BAG air-abrasion of SA titanium surface has been shown to decrease the surface roughness, enhance wettability, increase the surface free energy, and promote osteoblast cell proliferation compared to non-abraded SA surfaces.[42] Therefore, the effect of bone healing around the dental implant cannot be explained solely by the antibacterial effect of BAG.

For the present study, mixed microbial infection of *F. nucleatum* and *P. gingivalis* was selected as a model to form experimental bacterial biofilm on the implant surface in laboratory conditions. Both microorganisms are actively involved in the initiation and progression of peri-implant infection.[7,8,13,43,44] The air-abrasion of implants with biofilm was performed extra-orally in an aerobic condition, potentially compromising the viability of bacteria used for biofilm formation. However, our previous study showed that *F. nucleatum* and *P. gingivalis* strains used in this study could survive in the growth media in the aerobic environment for the time needed to perform the air-abrasion process.[25]

It is worth mentioning that the surface topography of dental implants differs among different manufacturers, and therefore certain surfaces may be more challenging to decontaminate, as indicated in animal studies.[45,46] In addition, biofilms associated with dental implant surfaces are multispecies and multilayered complex structures. Therefore, the possibility that a biofilm consisting of another consortium of bacteria would not be efficiently eradicated from the implants cannot be excluded. Accordingly, the results reported in the current study cannot be generalized and are valid for the *F. nucleatum* and *P. gingivalis* dual-species biofilm formed SA titanium implants. Nevertheless, sandblasting and acid etching are widely used in implant dentistry, and the bacterial species used for dual biofilm formation are strongly associated with periodontal and peri-implant diseases.[7,8,13,43,44]

Sun and colleagues developed a PI model in the rat in which the induction of the disease was performed after 1 week of the implant placement by infusing bacterial suspension containing *Streptococcus oralis* and *Aggregatibacter actinomycetomcomitans* for 3 months.[34] In another PI rat model described by Koutouzis and his co-workers, the PI was induced after 1 week of placing the healing abutment by 24 gingival lavages using polymicrobial inocula consisting of *P. gingivalis*, *T. denticola*, and *T. forsythia* for 12 weeks.[33] However, the model used in the current study shows that the *F. nucleatum* and *P. gingivalis* dual biofilm could trigger an inflammatory response that resulted in extensive PI with advanced bone resorption and extensive inflammation in the intact biofilm group. Furthermore, this model has advantages over other experimental PI models, such as ligature-induced and polymicrobial inoculation. It allows for the standardization of the defect size configuration among the experimental groups compared to the abovementioned models. In addition, the length of the experiment is shorter; therefore, less possible suffering for experimental animals.

The implants used in this study were 3.0 mm in length; however, the histomorphometric measurements were performed in the coronal 1 mm bone defect. The apical 2 mm of the implants were not analyzed because, in most implants, the apical part of the implants penetrated the maxillary sinuses. Shorter implants with a marginal bone defect can compromise their initial stability and affect healing. Therefore, in the present study, good initial stability was obtained using 3 mm long implants by engaging or partially penetrating the cortical bone of the maxillary sinus floor. Nevertheless, 2 mm and 4 mm implant lengths were also used in similar experiments.[33,34] Three implants with intact biofilm failed to osseointegrate and showed extensive PI with advanced bone resorption. The other three implants were lost during the healing period. This indicates that the dual biofilm used in this study could induce an inflammatory response and hinder bone healing around the infected implants.

Although the model used in this study allows to evaluate the healing of experimentally induced bone defects around implants, small-sized animals like rats have some limitations. The "critical size defect" in small animals would probably not provide much insight into the effect size in the human clinical situation. In this regard, skeletally large animals, such as dogs, may provide more clinically relevant information.[47] In addition, a small animal size is usually allowed for a limited number of experimental sites per animal. However, the use of small size animals has several advantages over skeletally large animals. It allows the use of large numbers of animals, thereby enabling sufficient data collection for analysis. Also, small animals have well-defined genetic backgrounds and minor variations in their biological response.

Moreover, they are more resistant to diseases, and thereby, the risk of animal loss during the experiments is reduced.[48]

In summary, the biofilm model used in this study could induce an inflammatory response and bone resorption, as demonstrated in the IB group. The use of BAG for biofilm air-abrasion (in the 45S5 and Zn4 groups) resulted in comparable bone regeneration as seen for sterile implants (the S group). Both BAG-treated groups showed more bone formation in the experimental defect area than seen for the inert group. Therefore, BAGs 45S5 or Zn4 can be considered promising materials for air-abrasion treatment of PI. In general, care should be taken when extrapolating the results of animal studies to the human clinical situation.

5 | CONCLUSIONS

This study presents evidence that using either 45S5 or ZnO-containing BAGs for air-abrasion of bacterial biofilm formed on sandblasted and acid-etched implant surfaces results in better osseointegration and bone regeneration compared to implants subjected to inert glass air-abrasion treatment.

AUTHOR CONTRIBUTIONS

Faleh Abushahba contributed to the methodology, performed surgical procedures, investigation, data curation, literature search, writing original draft, and editing the article. **Nagat Areid** contributed to surgical procedures, investigation, data curation, and editing the article. **Mervi Gürsoy** contributed to the methodology, dual biofilm formation, investigation, writing, editing, and critical review of the article. **Jaana Willberg** contributed to investigation, visualization of histological slides, editing, and critical review of the article. **Varpu Laine** contributed to the animal's anesthesia and post-operative care, editing, and critical review of the article. **Emrah Yatkin** contributed to the animal's anesthesia and post-operative care, editing, and critical review of the article. **Leena Hupa** contributed to the investigation, editing, and critical review of the article. **Timo O. Närhi** contributed to the conceptualization, methodology, supervision, reviewing, writing, editing, and critical review of the article. All authors approved the final version of this article.

ACKNOWLEDGMENTS

This study was supported by State Research Funding (grant number: ERVA50036). The authors thank the Biomedical research technicians Oona Hällfors and Mariia Valkama for their technical assistance in the laboratory. The authors also thank the Central Animal Laboratory of the University of Turku personnel, Siru Aaltola, and Terhi Hiltula-Maisala for expert animal care.

CONFLICT OF INTEREST

The authors declare that this paper is original and has no conflict of interest.

DATA AVAILABILITY STATEMENT

The data that support the findings of this study are available from the corresponding author upon reasonable request.

ORCID

Faleh Abushahba https://orcid.org/0000-0002-8032-9396

REFERENCES

1. Derks J, Tomasi C. Peri-implant health and disease. A systematic review of current epidemiology. *J Clin Periodontol*. 2015;42(Suppl 16):S158-S171. doi:10.1111/jcpe.12334
2. Salvi GE, Cosgarea R, Sculean A. Prevalence and mechanisms of peri-implant diseases. *J Dent Res*. 2017;96(1):31-37. doi:10.1177/0022034516667484
3. Berglundh T, Armitage G, Araujo MG, et al. Peri-implant diseases and conditions: consensus report of workgroup 4 of the 2017 world workshop on the classification of periodontal and peri-implant diseases and conditions. *J Clin Periodontol*. 2018;45(Suppl 20):S286-S291. doi:10.1111/jcpe.12957
4. Renvert S, Persson GR, Pirih FQ, Camargo PM. Peri-implant health, peri-implant mucositis, and peri-implantitis: case definitions and diagnostic considerations. *J Clin Periodontol*. 2018;45(Suppl 20):S278-S285. doi:10.1111/jcpe.12956
5. Schwarz F, Derks J, Monje A, Wang HL. Peri-implantitis. *J Periodontol*. 2018;89(Suppl 1):S267-S290. doi:10.1002/JPER.16-0350
6. Suarez F, Monje A, Galindo-Moreno P, Wang HL. Implant surface detoxification: a comprehensive review. *Implant Dent*. 2013;22(5):465-473. doi:10.1097/ID.0b013e3182a2b8f4
7. Belibasakis GN, Manoil D. Microbial community-driven etiopathogenesis of peri-implantitis. *J Dent Res*. 2021;100(1):21-28. doi:10.1177/0022034520949851
8. Casado PL, Otazu IB, Balduino A, de Mello W, Barboza EP, Duarte ME. Identification of periodontal pathogens in healthy periimplant sites. *Implant Dent*. 2011;20(3):226-235. doi:10.1097/ID.0b013e3182199348
9. Chen Y, Shi T, Li Y, Huang L, Yin D. *Fusobacterium nucleatum*: the opportunistic pathogen of periodontal and peri-implant diseases. *Front Microbiol*. 2022;13:860149. doi:10.3389/fmicb.2022.860149
10. Diaz PI, Zilm PS, Rogers AH. Fusobacterium nucleatum supports the growth of *Porphyromonas gingivalis* in oxygenated and carbon-dioxide-depleted environments. *Microbiology (Reading)*. 2002;148(Pt 2):467-472. doi:10.1099/00221287-148-2-467
11. Hajishengallis G, Darveau RP, Curtis MA. The keystone-pathogen hypothesis. *Nat Rev Microbiol*. 2012;10(10):717-725. doi:10.1038/nrmicro2873
12. Lee A, Wang HL. Biofilm related to dental implants. *Implant Dent*. 2010;19(5):387-393. doi:10.1097/ID.0b013e3181effa53
13. Zhuang LF, Watt RM, Mattheos N, Si MS, Lai HC, Lang NP. Periodontal and peri-implant microbiota in patients with healthy and inflamed periodontal and peri-implant tissues. *Clin Oral Implants Res*. 2016;27(1):13-21. doi:10.1111/clr.12508
14. Teughels W, Van Assche N, Sliepen I, Quirynen M. Effect of material characteristics and/or surface topography on biofilm development. *Clin Oral Implants Res*. 2006;17(Suppl 2):68-81. doi:10.1111/j.1600-0501.2006.01353.x
15. Estefanía-Fresco R, García-de-la-Fuente AM, Egaña-Fernández-Valderrama A, Bravo M, Aguirre-Zorzano LA. One-year results of a nonsurgical treatment protocol for peri-implantitis. A retrospective case series. *Clin Oral Implants Res*. 2019;30(7):702-712. doi:10.1111/clr.13456
16. Heitz-Mayfield LJ, Mombelli A. The therapy of peri-implantitis: a systematic review. *Int J Oral Maxillofac Implants*. 2014;29:325-345. doi:10.11607/jomi.2014suppl.g5.3
17. Ramanauskaite A, Fretwurst T, Schwarz F. Efficacy of alternative or adjunctive measures to conventional non-surgical and surgical treatment of peri-implant mucositis and peri-implantitis: a systematic review and meta-analysis. *Int J Implant Dent*. 2021;7(1):112. doi:10.1186/s40729-021-00388-x

18. Esposito M, Grusovin MG, Tzanetea E, Piattelli A, Worthington HV. Interventions for replacing missing teeth: treatment of perimplantitis. *Cochrane Database Syst Rev*. 2010;6:CD004970. doi:10.1002/14651858.CD004970.pub4
19. Keim D, Nickles K, Dannewitz B, Ratka C, Eickholz P, Petsos H. In vitro efficacy of three different implant surface decontamination methods in three different defect configurations. *Clin Oral Implants Res*. 2019;30(6):550-558. doi:10.1111/clr.13441
20. Sahrmann P, Ronay V, Hofer D, Attin T, Jung RE, Schmidlin PR. In vitro cleaning potential of three different implant debridement methods. *Clin Oral Implants Res*. 2015;26(3):314-319. doi:10.1111/clr.12322
21. Banerjee A, Hajatdoost-Sani M, Farrell S, Thompson I. A clinical evaluation and comparison of bioactive glass and sodium bicarbonate air-polishing powders. *J Dent*. 2010;38(6):475-479. doi:10.1016/j.jdent.2010.03.001
22. Koller G, Cook RJ, Thompson ID, Watson TF, Di Silvio L. Surface modification of titanium implants using bioactive glasses with air abrasion technologies. *J Mater Sci Mater Med*. 2007;18(12):2291-2296. doi:10.1007/s10856-007-3137-z
23. Petersilka GJ, Steinmann D, Häberlein I, Heinecke A, Flemmig TF. Subgingival plaque removal in buccal and lingual sites using a novel low abrasive air-polishing powder. *J Clin Periodontol*. 2003;30(4):328-333. doi:10.1034/j.1600-051x.2003.00290.x
24. Abushahba F, Söderling E, Aalto-Setälä L, Hupa L, Närhi TO. Air abrasion with bioactive glass eradicates *Streptococcus mutans* biofilm from a sandblasted and acid-etched titanium surface. *J Oral Implantol*. 2019;45(6):444-450. doi:10.1563/aaid-joi-D-18-00324
25. Abushahba F, Gürsoy M, Hupa L, Närhi TO. Effect of bioactive glass air-abrasion on fusobacterium nucleatum and *Porphyromonas gingivalis* biofilm formed on moderately rough titanium surface. *Eur J Oral Sci*. 2021;129(3):e12783. doi:10.1111/eos.12783
26. Allan I, Newman H, Wilson M. Antibacterial activity of particulate bioglass against supra- and subgingival bacteria. *Biomaterials*. 2001;22(12):1683-1687. doi:10.1016/s0142-9612(00)00330-6
27. Allan I, Newman H, Wilson M. Particulate bioglass reduces the viability of bacterial biofilms formed on its surface in an in vitro model. *Clin Oral Implants Res*. 2002;13(1):53-58. doi:10.1034/j.1600-0501.2002.130106.x
28. Stoor P, Söderling E, Salonen JI. Antibacterial effects of a bioactive glass paste on oral microorganisms. *Acta Odontol Scand*. 1998;56(3):161-165. doi:10.1080/000163598422901
29. Hench LL. The story of bioglass. *J Mater Sci Mater Med*. 2006;17(11):967-978. doi:10.1007/s10856-006-0432-z
30. Wetzel R, Blochberger M, Scheffler F, Hupa L, Brauer DS. Mg or Zn for Ca substitution improves the sintering of bioglass 45S5. *Sci Rep*. 2020;10(1):15964. doi:10.1038/s41598-020-72091-7
31. Abushahba F, Söderling E, Aalto-Setälä L, Sangder J, Hupa L, Närhi TO. Antibacterial properties of bioactive glass particle abraded titanium against *Streptococcus mutans*. *Biomed Phys Eng Express*. 2018;4:045002. doi:10.1088/2057-1976/aabeee
32. Yamamoto O. Influence of particle size on the antibacterial activity of zinc oxide. *Int J Inorg Mater*. 2001;3(7):643-646. doi:10.1016/S1466-6049(01)00197-0
33. Koutouzis T, Eastman C, Chukkapalli S, Larjava H, Kesavalu L. A novel rat model of polymicrobial peri-implantitis: a preliminary study. *J Periodontol*. 2017;88(2):e32-e41. doi:10.1902/jop.2016.160273
34. Sun J, Eberhard J, Glage S, et al. Development of a peri-implantitis model in the rat. *Clin Oral Implants Res*. 2020;31(3):203-214. doi:10.1111/clr.13556
35. Charan J, Kantharia ND. How to calculate sample size in animal studies? *J Pharmacol Pharmacother*. 2013;4(4):303-306. doi:10.4103/0976-500X.119726
36. Collier FM, Huang WH, Holloway WR, et al. Osteoclasts from human giant cell tumors of bone lack estrogen receptors. *Endocrinology*. 1998;139(3):1258-1267. doi:10.1210/endo.139.3.5825
37. Ishikawa K, Miyamoto Y, Yuasa T, Ito A, Nagayama M, Suzuki K. Fabrication of Zn containing apatite cement and its initial evaluation using human osteoblastic cells. *Biomaterials*. 2002;23(2):423-428. doi:10.1016/s0142-9612(01)00121-1
38. Li H, Chang J. Bioactive silicate materials stimulate angiogenesis in fibroblast and endothelial cell co-culture system through paracrine effect [published correction appears in *Acta biomater*. 2019 Aug; 94:646]. *Acta Biomater*. 2013;9(6):6981-6991. doi:10.1016/j.actbio.2013.02.014
39. Xynos ID, Edgar AJ, Buttery LD, Hench LL, Polak JM. Ionic products of bioactive glass dissolution increase proliferation of human osteoblasts and induce insulin-like growth factor II mRNA expression and protein synthesis. *Biochem Biophys Res Commun*. 2000;276(2):461-465. doi:10.1006/bbrc.2000.3503
40. Hu S, Chang J, Liu M, Ning C. Study on antibacterial effect of 45S5 bioglass. *J Mater Sci Mater Med*. 2009;20(1):281-286. doi:10.1007/s10856-008-3564-5
41. Blochberger M, Hupa L, Brauer DS. Influence of zinc and magnesium substitution on ion release from bioglass 45S5 at physiological and acidic pH. *Biomed Glasses*. 2015;1(1):93-107. doi:10.1515/bglass-2015-0009
42. Abushahba F, Tuukkanen J, Aalto-Setälä L, Miinalainen I, Hupa L, Närhi TO. Effect of bioactive glass air-abrasion on the wettability and osteoblast proliferation on sandblasted and acid-etched titanium surfaces. *Eur J Oral Sci*. 2020;128(2):160-169. doi:10.1111/eos.12683
43. Al-Ahmad A, Muzafferiy F, Anderson AC, et al. Shift of microbial composition of peri-implantitis-associated oral biofilm as revealed by 16 S rRNA gene cloning. *J Med Microbiol*. 2018;67(3):332-340. doi:10.1099/jmm.0.000682
44. Okamoto AC, Gaetti-Jardim E, Cai S, Avila-Campos MJ. Influence of antimicrobial subinhibitory concentrations on hemolytic activity and bacteriocin-like substances in oral *Fusobacterium nucleatum*. *New Microbiol*. 2000;23(2):137-142.
45. Albouy JP, Abrahamsson I, Persson LG, Berglundh T. Implant surface characteristics influence the outcome of treatment of peri-implantitis: an experimental study in dogs. *J Clin Periodontol*. 2011;38(1):58-64. doi:10.1111/j.1600-051X.2010.01631.x
46. Albouy JP, Abrahamsson I, Berglundh T. Spontaneous progression of experimental peri-implantitis at implants with different surface characteristics: an experimental study in dogs. *J Clin Periodontol*. 2012;39(2):182-187. doi:10.1111/j.1600-051X.2011.01820.x
47. Araújo MG, Lindhe J. Dimensional ridge alterations following tooth extraction. An experimental study in the dog. *J Clin Periodontol*. 2005;32(2):212-218. doi:10.1111/j.1600-051X.2005.00642.x
48. Stavropoulos A, Sculean A, Bosshardt DD, Buser D, Klinge B. Pre-clinical in vivo models for the screening of bone biomaterials for oral/craniofacial indications: focus on small-animal models. *Periodontol 2000*. 2000;68(1):55-65. doi:10.1111/prd.12065

How to cite this article: Abushahba F, Areid N, Gürsoy M, et al. Bioactive glass air-abrasion promotes healing around contaminated implant surfaces surrounded by circumferential bone defects: An experimental study in the rat. *Clin Implant Dent Relat Res*. 2023;1-10. doi:10.1111/cid.13172